Journal of Scientific Computing (2023) 94:37
https://doi.org/10.1007/s10915-022-02093-2

An Efficient Adaptive Mesh Redistribution Method for Nonlinear Eigenvalue Problems in Bose–Einstein Condensates

Hehu Xie[1,2] · **Manting Xie**[3] · **Xiaobo Yin**[4] · **Gang Zhao**[1,2]

Received: 23 August 2021 / Revised: 11 December 2022 / Accepted: 24 December 2022

Abstract
We design a multilevel correction type of adaptive finite element method based on the moving mesh technique for solving nonlinear eigenvalue problems. In this paper, we take the ground state of Bose–Einstein condensates as the example of a nonlinear eigenvalue problem to show the solving process. For this aim, we propose a non-nested augmented subspace method for the nonlinear eigenvalue problems since the sequence of finite element spaces generated by the r-adaptive method has non-nested property. The new method proposed in this paper can improve the efficiency for solving nonlinear eigenvalue problems by the corresponding theoretical analysis and numerical examples.

Keywords Nonlinear eigenvalue problem · Bose–Einstein condensates · Non-nested augmented subspace method · Tensor technique · Moving mesh

Mathematics Subject Classification 65N30 · 65N25 · 65L15 · 65B99

✉ Manting Xie
mtxie@tju.edu.cn

Hehu Xie
hhxie@lsec.cc.ac.cn

Xiaobo Yin
yinxb@mail.ccnu.edu.cn

Gang Zhao
zhaog6@lsec.cc.ac.cn

[1] LSEC, NCMIS, Institute of Computational Mathematics, Academy of Mathematics and Systems Science, Chinese Academy of Sciences, Beijing 100190, China

[2] School of Mathematical Sciences, University of Chinese Academy of Sciences, Beijing 100049, China

[3] Center for Applied Mathematics, Tianjin University, Tianjin 300072, China

[4] School of Mathematics and Statistics and Hubei Key Laboratory of Mathematical Sciences, Central China Normal University, Wuhan 430079, China

Published online: 06 January 2023

1 Introduction

There exist many nonlinear eigenvalue problems in quantum mechanics, electronic structure, etc. It demands research about efficient numerical methods for solving nonlinear eigenvalue problems. As an example, we consider the numerical methods for computing the ground state solution of Bose–Einstein condensates which comes from the quantum theory and is written as a nonlinear eigenvalue problem. Quantum theory is one of the most important scientific discoveries in the last century, which asserts that all objects behave like waves on a micro-scale. However, the extremely small wavelength makes it difficult to observe the quantum phenomenon. Now, the realization of a new state of matter called "the fifth state of matter"—Bose–Einstein condensates (BECs) makes it possible to explore the quantum world in experiments. At the critical temperature (near absolute zero), some Bosons will occupy the same quantum state, thus forming the observable BECs. It is worth mentioning that the 2001 Nobel Prize in Physics was awarded to three scientists who first realized BECs [4, 24].

In the past 20 years, especially after the realization of BECs, related research has developed rapidly, and mathematical modeling and numerical simulation play a very important role, in theory, prediction, and experimental guidance. For the numerical study of ground states of BEC, computational mathematicians and physicists are more interested in effective and accurate numerical simulations. Bao et al. [8–10] proposed normalized gradient flow method to obtain ground state, a type of efficient Sobolev gradient method is proposed in [21] and [26]. Heid et al. [28] designed an adaptive finite element gradient flow method for the energy minimization aspect. Li et al. [35] proposed a combined discontinuous Galerkin (DG) method based on the imaginary-time method. In [21], Danaila and Hecht proposed an adaptive finite element method based on imaginary time and Sobolev gradient flow methods. Wu et al. [41] studied the regularized Newton method and showed its efficiency and robustness. Danaila and Protas [22] proposed unconstrained optimization methods on Riemannian manifolds. In [5, 6], Antoine et al. designed a type of preconditioned nonlinear conjugate gradient method to compute the stationary states of rotating Bose–Einstein condensates.

At the critical temperature (near absolute zero), the macroscopic behavior of the BECs can be described by the wave function $\psi(\mathbf{x}, t)$ which is determined by the dimensionless Gross-Pitaevskii equation (GPE) in $\mathbb{R}^d$ $(d = 1, 2, 3)$ [8–10]

$$\mathrm{i}\,\partial_t \psi(\mathbf{x}, t) = \left[-\frac{1}{2}\nabla^2 + W(\mathbf{x}) + \zeta|\psi|^2\right]\psi(\mathbf{x}, t), \qquad \mathbf{x} \in \mathbb{R}^d, \quad t > 0, \tag{1.1}$$

and the initial value

$$\psi(\mathbf{x}, t = 0) = \psi_0(\mathbf{x}), \qquad \mathbf{x} \in \mathbb{R}^d, \tag{1.2}$$

where $\mathrm{i} = \sqrt{-1}$ is the imaginary unit, t is time, $\mathbf{x} = (x, y)^T \in \mathbb{R}^2$ or $\mathbf{x} = (x, y, z)^T \in \mathbb{R}^3$, $V(\mathbf{x})$ denotes a given real-valued external trapping potential which is determined by the type of system under investigation, ζ is a dimensionless interaction constant (positive for repulsive interaction and negative for attractive interaction). If we consider the external potential $W(x)$ that is measurable and locally bounded and $\lim_{|\mathbf{x}|\to\infty} W(\mathbf{x}) = \infty$, then the wave function ψ vanishes exponentially fast as $|\mathbf{x}| \to \infty$ [36]. Therefore, it is reasonable to truncate the problem (1.1)–(1.2) into a bounded computational domain Ω with cone property and homogeneous Dirichlet boundary condition.

To find ground states of BEC, inserting $\psi(\mathbf{x}, t) = e^{i\lambda t}u(\mathbf{x})$ into (1.1) gives the following nonlinear eigenvalue problem (NLEP):

$$\begin{cases} -\frac{1}{2}\nabla^2 u + Wu + \zeta|u|^2 u = \lambda u, & \text{in } \Omega, \\ u = 0, & \text{on } \partial\Omega, \\ \int_\Omega |u|^2 \mathrm{d}\Omega = 1, \end{cases} \tag{1.3}$$

where the eigenvalue λ is the chemical potential of the condensate, and the eigenfunction $u(\mathbf{x})$ is a real wavefunction. For generality, we consider the problem (1.3) on the general domain Ω. The the problem (1.3) may has the singularities from the domains. As we all know, the ground state of BEC is actually the eigenfunction corresponding to the minimum eigenvalue of the NLEP (1.3). For simplicity of notation, we also call the solution of the problem (1.3) as the ground state of BEC. Hence, in this paper, we focus on the efficient numerical method for the NLEP (1.3).

The energy can be given by

$$E(u) = \int_\Omega \left(\frac{1}{2}|\nabla u(\mathbf{x})|^2 + W(\mathbf{x})|u(\mathbf{x})|^2 + \frac{\zeta}{2}|u(\mathbf{x})|^4 \right) \mathrm{d}\mathbf{x}. \tag{1.4}$$

Hence, the eigenvalue λ can be computed from the corresponding eigenfunction as

$$\lambda = \int_\Omega \left(\frac{1}{2}|\nabla u(\mathbf{x})|^2 + W(\mathbf{x})|u(\mathbf{x})|^2 + \zeta|u(\mathbf{x})|^4 \right) \mathrm{d}\mathbf{x} = E(u) + \int_\Omega \frac{\zeta}{2}|u(\mathbf{x})|^4 \mathrm{d}\mathbf{x}. \tag{1.5}$$

Solving the NLEP (1.3) has attracted the attention of many researchers, and has led to many important studies. In [48], Zhou gave the convergence analysis of the finite-dimensional approximation for the ground state solution of Bose–Einstein condensates. Cancès et al. [14] presented the a priori error estimates and error bounds for the ground state solution of Bose–Einstein condensates by the finite dimensional approximation. Two grid schemes based on the spectral method, finite difference method, and finite element method were studied in [16], [19] and [18], respectively. The a posteriori estimator for the plane waves discretization was studied in [15]. Based on the computable errors, Xie et al. [45] obtained the asymptotic lower bound of the ground state energy. Based on the plane-wave method, an adaptive method has been proposed to solve the ground state solution by Cancès et al. [16]. The inexact Newton method based on spectral collocation was studied in [17]. Jeng et al. studied the spectral collocation method and the two-level continuous scheme in [32]. [46] proposed a type of cascadic adaptive FEM for solving NLEPs.

It is well known that the adaptive method could improve the computational efficiency when solving partial differential equations [13, 30, 31, 38, 40]. There are three types of important adaptive methods: the *h*-adaptive methods which locally refine or coarsen the mesh, the *p*-adaptive methods which locally enrich the order of the approximate polynomial, and the *r*-adaptive methods which redistribute the grid points while keeping the number of mesh grids unchanged. The *r*-adaptive method is also called the moving mesh method, which has been successfully used in many fields such as the computational fluid dynamics [38, 39], phase-field model [12, 40], reaction-diffusion models [31], unstable flow in porous media [30] and Kohn-Sham equation [11]. The first aim of this paper is to design an adaptive method based on a mesh redistributed technique to solve the ground state solution of BECs. However, we do not require the number of mesh grids unchanged during the mesh redistributing process. In the framework of the moving mesh method, the so-called monitor function is of particular

importance since it is used to control the movement of the mesh grids. In this paper, the default monitor function given by Mshmet is used (Section 4.2 in [3] and Section 2.4 in [25]).

In recent years, based on the multilevel correction method and augmented subspace method [37, 42], Xie et al. proposed a type of multigrid method for solving the ground state solution of BECs [33, 43, 44]. Based on the numerical method in [44], Zhang et al. propose an efficient multigrid method [47] with a tensor assembling technique. This method's interesting and important property is that the asymptotic computational work does not depend on the number of nonlinear iterations. The second aim of this paper is to design the multilevel correction algorithm on the sequence of meshes generated by the moving mesh method. The existed multilevel correction method, like [33, 37, 42–44, 47], requires the condition that the low-dimensional finite element space is a subspace of the high-dimensional finite element space. However, this condition is not satisfied by the sequence of finite element spaces generated by the moving mesh method. In this paper, to apply the multilevel correction algorithm on the sequence of finite element spaces generated by the moving mesh method, we design a non-nested augmented subspace method for solving the NLEP (1.3), and then an efficient multilevel correction method for computing the ground state of BECs.

An outline of the paper goes as follows. In Section 2, we introduce finite element method for the nonlinear eigenvalue problem (1.3). The non-nested augmented subspace method for the nonlinear eigenvalue problem is given in Section 3. Section 4 is devoted to designing the multilevel correction algorithm on the sequence of meshes generated by the moving mesh method. Some numerical examples are provided in Section 5 to validate the convergence and computational complexity of the proposed numerical method. Some concluding remarks are given in the last section.

2 Finite Element Method for the NLEP

This section is devoted to introducing some notation and the finite element method for the NLEP (1.3). The letter C (with or without subscripts) denotes a generic positive constant which may be different at its different occurrences. For convenience, the symbols $\lesssim$, $\gtrsim$ and $\approx$ will be used in this paper. That $x_1 \lesssim y_1, x_2 \gtrsim y_2$ and $x_3 \approx y_3$, mean that $x_1 \leq C_1 y_1$, $x_2 \geq c_2 y_2$ and $c_3 x_3 \leq y_3 \leq C_3 x_3$ for some constants C_1, c_2, c_3 and C_3 that are independent of mesh sizes. The standard notation for the Sobolev spaces $W^{s,p}(\Omega)$ and their associated norms $\|\cdot\|_{s,p,\Omega}$ and seminorms $|\cdot|_{s,p,\Omega}$ (see, e.g., [1]) will be used. For $p = 2$, we denote $H^s(\Omega) = W^{s,2}(\Omega)$ and $H_0^1(\Omega) = \{v \in H^1(\Omega) : v|_{\partial\Omega} = 0\}$, where $v|_{\partial\Omega} = 0$ is in the sense of trace, $\|\cdot\|_{s,\Omega} = \|\cdot\|_{s,2,\Omega}$. In this paper, we set $V := \{v \in H_0^1(\Omega) \mid E(v) < \infty\}$ and use $\|\cdot\|_s$ to denote $\|\cdot\|_{s,\Omega}$ for simplicity. The $L^2(\Omega)$ inner-product is denoted by $(\cdot,\cdot)$, that is

$$(v, w) := \int_\Omega vw \mathrm{d}\Omega, \quad \forall v, w \in L^2(\Omega).$$

For the aim of finite element discretization, we define the corresponding weak form for (1.3) as follows: Find $(\lambda, u) \in \mathbb{R} \times V$ such that $\|u\|_0^2 = 1, u \geq 0$, and

$$\widehat{a}(u, v) = \lambda b(u, v), \quad \forall v \in V, \tag{2.1}$$

where

$$\widehat{a}(u, v) := a(u, v) + (\zeta |u|^2 u, v), \quad b(u, v) := (u, v), \tag{2.2}$$

$$a(u, v) := \frac{1}{2}(\nabla u, \nabla v) + (Wu, v). \tag{2.3}$$

Obviously, $a(\cdot, \cdot)$ satisfies

$$c_a \|w\|_{1,\Omega} \leq \|w\|_{a,\Omega} \leq C_a \|w\|_{1,\Omega},$$

where $\|\cdot\|_{a,\Omega}$ is the energy norm defined by $\|w\|_{a,\Omega} = \sqrt{a(w, w)}$. Now, let us define the finite element method [13, 20] for the problem (2.1). First, we divide the computational domain $\Omega \subset \mathbb{R}^d$ into cells (triangles or rectangles for $d = 2$, tetrahedrons or hexahedrons for $d = 3$). The diameter of a cell $K \in \mathcal{T}_h$ is denoted by h_K and define h as $h := \max_{K\in\mathcal{T}_h} h_K$. Then the corresponding linear finite element space $V_h \subset V$ can be built on the mesh $\mathcal{T}_h$, i.e.,

$$V_h := \left\{ v_h \in H_0^1(\Omega) \;\middle|\; v_h|_K \in \mathcal{P}_1, \ \forall K \in \mathcal{T}_h \right\} \cap H_0^1(\Omega), \tag{2.4}$$

where $\mathcal{P}_1$ denotes the linear polynomial space and V_h is a family of finite-dimensional spaces that satisfy the following assumption:

$$\lim_{h\to 0} \inf_{v_h\in V_h} \|w - v_h\|_{a,\Omega} = 0, \quad \forall w \in V. \tag{2.5}$$

Based on the linear space V_h, we can discretize (2.1) as follows: Find $(\bar{\lambda}_h, \bar{u}_h) \in \mathbb{R} \times V_h$ such that $\|\bar{u}_h\|_0^2 = 1$, $\bar{u}_h \geq 0$, and

$$\widehat{a}(\bar{u}_h, v_h) = \bar{\lambda}_h b(\bar{u}_h, v_h), \quad \forall v_h \in V_h. \tag{2.6}$$

Then, the discrete ground state energy is given by

$$E(\bar{u}_h) = \int_\Omega \left(\frac{1}{2}|\nabla \bar{u}_h|^2 + W|\bar{u}_h|^2 + \frac{\zeta}{2}|\bar{u}_h|^4 \right) \mathrm{d}\Omega. \tag{2.7}$$

For the following analysis, let us define the Galerkin projection $P_h : H_0^1(\Omega) \to V_h$ by

$$a(u - P_h u, v_h) = 0 \quad \forall v_h \in V_h. \tag{2.8}$$

It is obvious that

$$\|P_h u\|_{a,\Omega} \leq \|u\|_{a,\Omega} \quad \forall u \in V. \tag{2.9}$$

To give the error estimates for the finite element method, we define the following notation

$$\delta_h(u) := \inf_{v_h\in V_h} \|u - v_h\|_{a,\Omega}. \tag{2.10}$$

Lemma 2.1 *([14, Theorem 1], [48]) There exists $h_0 > 0$ such that for all $0 < h < h_0$, the principal eigenpair $(\lambda, u) \in \mathbb{R} \times V$ and its approximation $(\bar{\lambda}_h, \bar{u}_h) \in \mathbb{R} \times X_h$ satisfy the following error estimates*

$$\|u - \bar{u}_h\|_{a,\Omega} \lesssim \delta_h(u), \tag{2.11}$$

$$\|u - \bar{u}_h\|_0 \lesssim \alpha_a(V_h)\|u - \bar{u}_h\|_{a,\Omega} \lesssim \alpha_a(V_h)\delta_h(u), \tag{2.12}$$

$$|\lambda - \bar{\lambda}_h| \lesssim \|u - \bar{u}_h\|_{a,\Omega}^2 + \|u - \bar{u}_h\|_0 \lesssim \rho(V_h)\|u - \bar{u}_h\|_{a,\Omega}, \tag{2.13}$$

where $\rho(V_h) := \alpha_a(V_h) + \delta_h(u)$, and $\alpha_a(V_h)$ is defined as follows:

$$\alpha_a(V_h) = \sup_{f\in L^2(\Omega), \|f\|_0=1} \inf_{v_h\in V_h} \|Tf - v_h\|_{a,\Omega}$$

with the operator T being defined as follows: Find $Tf \in u^{\perp}$ such that

$$\langle (E''(u) - \lambda)Tf, v\rangle = (f, v), \quad \forall v \in u^{\perp},$$

where $E''(u)$ is the second derivative of E at u, and $u^{\perp} = \{v \in V : |\int_{\Omega} uv d\Omega = 0\}$.

Based on (1.5), Lemma 2.1, the Hölder inequality, and the triangle inequality, we have the following corollary.

Corollary 2.1 *Under the conditions of Lemma 2.1, $E = E(u)$ and its approximation $\bar{E}_h = E(\bar{u}_h)$ satisfy the following error estimates*

$$|E - E_h| \lesssim |\lambda - \bar{\lambda}_h| + \|u - \bar{u}_h\|_0 \lesssim \rho(V_h)\|u - \bar{u}_h\|_{a,\Omega}. \tag{2.14}$$

Corollary 2.2 *Under the conditions of Lemma 2.1, we have the following finer error estimate*

$$\|u - \bar{u}_h\|_a \leq \frac{1}{1 - C\rho(V_h)}\delta_h(u), \tag{2.15}$$

where the constant C is independent of the mesh size.

Proof From the definition (2.8) of finite element projection P_h and the standard finite element error estimate [13, 20], we have

$$\|u - P_h u\|_a = \inf_{v_h \in V_h} \|u - v_h\|_a, \quad \|u - P_h u\|_0 \leq \rho(V_h)\|u - P_h u\|_a. \tag{2.16}$$

Set $w_h = u_h - P_h u \in V_h \subset V$. Combing (2.1), (2.6), (2.8) and the triangle inequality, the following error estimates hold

$$\begin{aligned}
a(\bar{u}_h - P_h u, w_h) &\leq a(\bar{u}_h - P_h u, w_h) + \int_{\Omega} \zeta |\bar{u}_h|^2 (\bar{u}_h - P_h u) w_h \mathrm{d}\Omega \\
&= b(\bar{\lambda}_h \bar{u}_h, w_h) - a(u, w_h) - \int_{\Omega} \zeta |\bar{u}_h|^2 P_h u w_h \mathrm{d}\Omega \\
&= b(\bar{\lambda}_h \bar{u}_h - \lambda u, w_h) + \int_{\Omega} \zeta \big(|u|^2 u - |\bar{u}_h|^2 P_h u\big) w_h \mathrm{d}\Omega \\
&= b(\bar{\lambda}_h \bar{u}_h - \lambda u, w_h) + \int_{\Omega} \zeta \big(|u|^2 - |\bar{u}_h|^2\big) u w_h \mathrm{d}\Omega + \int_{\Omega} \zeta |\bar{u}_h|^2 \big(u - P_h u\big) w_h \mathrm{d}\Omega \\
&= \|\bar{\lambda}_h \bar{u}_h - \lambda u\|_0 \|w_h\|_0 + \int_{\Omega} \zeta \big(|u|^2 - |\bar{u}_h|^2\big) u w_h \mathrm{d}\Omega + \int_{\Omega} \zeta |\bar{u}_h|^2 \big(u - P_h u\big) w_h \mathrm{d}\Omega.
\end{aligned} \tag{2.17}$$

For the second term of (2.17), using the Hölder inequality, we have

$$\begin{aligned}
\int_{\Omega} \zeta \big(|u|^2 - |\bar{u}_h|^2\big) u w_h \mathrm{d}\Omega &= \int_{\Omega} \zeta \big(u + \bar{u}_h\big)\big(u - \bar{u}_h\big) u w_h \mathrm{d}\Omega \\
&\leq \zeta \left(\int_{\Omega} |u + \bar{u}_h|^6 \mathrm{d}\Omega\right)^{1/6} \left(\int_{\Omega} |u - \bar{u}_h|^2 \mathrm{d}\Omega\right)^{1/2} \left(\int_{\Omega} |u|^6 \mathrm{d}\Omega\right)^{1/6} \left(\int_{\Omega} |w_h|^6 \mathrm{d}\Omega\right)^{1/6} \\
&\leq \zeta \|u + \bar{u}_h\|_{0,6} \|u\|_{0,6} \|u - \bar{u}_h\|_0 \|w_h\|_{0,6}.
\end{aligned} \tag{2.18}$$

From Sobolev imbedding theorem (cf. [1])

$$W^{s,p}(\Omega) \hookrightarrow L^q(\Omega), \text{ for } p \leq q \leq p^* = dp/(d - sp), \ \Omega \subset \mathbb{R}^d,$$

we have

$$\|v\|_{0,6} \leq C_\Omega \|v\|_a, \ \forall v \in V, \ \text{for } d = 2, 3, \tag{2.19}$$

where C_Ω is a constant depending only on Ω.

Then, the combination of (2.18) and (2.19) leads to

$$\int_\Omega \zeta \left(|u|^2 - |\bar{u}_h|^2\right) u w_h \mathrm{d}\Omega \leq C_1 \|u - \bar{u}_h\|_0 \|w_h\|_a, \tag{2.20}$$

where $C_1 = C_\Omega^3 \zeta (\|u\|_a + \|\bar{u}_h\|_a)\|u\|_a$.

In the same way, for the second term of (2.17), we have

$$\int_\Omega \zeta |\bar{u}_h|^2 \left(u - P_h u\right) w_h \mathrm{d}\Omega \leq C_2 \|u - P_h u\|_0 \|w_h\|_a, \tag{2.21}$$

where $C_2 = C_\Omega^3 \zeta \|\bar{u}_h\|_a^2$.

Combing (2.16), (2.17), (2.20), (2.21), and Lemma 2.1, we have

$$\begin{aligned} \|\bar{u}_h - P_h u\|_a &\leq \|\bar{u}_h\|_0 |\lambda - \bar{\lambda}_h| + (C_1 + |\lambda|)\|u - \bar{u}_h\|_0 + C_2 \|u - P_h u\|_0 \\ &\leq C \rho(V_h) \|u - \bar{u}_h\|_a, \end{aligned} \tag{2.22}$$

where the constant C depends on C_1 and C_2, but is independent of the mesh size.

From (2.22) and the triangle inequality, the following estimates hold

$$\begin{aligned} \|u - \bar{u}_h\|_a &\leq \|u - P_h u\|_a + \|P_h u - \bar{u}_h\|_a \\ &\leq \|u - P_h u\|_a + C \rho(V_h) \|u - \bar{u}_h\|_a. \end{aligned}$$

This is the desired (2.15) and the proof is completed. □

3 Non-nested Augmented Subspace Method

In this section, we design a non-nested augmented subspace method based on a non-nested coarse finite element space. With the help of the low-dimensional augmented subspace, the method can transform the solution of a nonlinear eigenvalue problem on the fine spaces into solving a linear boundary value problem of the same scale, and a small-scale eigenvalue problem in a low-dimensional subspace. Different from the existing augmented subspace or multilevel correction scheme (c.f. [33, 37, 42, 44, 47]), the coarse space constructed in this article is not the subspace of the finer finite element space which gives the feasibility to use the augmented subspace method on the of meshes that are generated by the moving mesh method. This section introduces the algorithm, efficient implementing techniques, and their theoretical analysis.

3.1 Non-nested Augmented Subspace Algorithm

We use a coarse mesh $\mathcal{T}_H$ with the mesh size H and define the coarse linear finite element space V_H on $\mathcal{T}_H$. The meshes $\mathcal{T}_H$ and $\mathcal{T}_h$ are not required to have a nested relationship. With the help of V_H, an augmented subspace of V_h is designed as $V_{H,h} := V_H + \mathrm{span}\{\widetilde{u}_h\}$, where $\widetilde{u}_h \in V_h$ is a finite element function defined on $\mathcal{T}_h$. Although V_H and V_h do not have the nested relationship which means $V_{H,h} \not\subset V_h$, however, $V_{H,h} \subset V$ does hold. Therefore, we could use the error estimates for $V_{H,h}$ in Lemma 2.1 and Corollary 2.2.

Before implementing the augmented subspace method, an approximation $(\lambda_h^{(\ell)}, u_h^{(\ell)})$ of the principal eigenpair (λ, u) is assumed to be available. The augmented subspace iteration algorithm (Algorithm 3.1) is used to improve the accuracy of $(\lambda_h^{(\ell)}, u_h^{(\ell)})$. Here the superscript ℓ denotes iteration index and $(\lambda_h^{(\ell)}, u_h^{(\ell)})$ is the input parameter of the algorithm, while $(\lambda_h^{(\ell+1)}, u_h^{(\ell+1)})$ is the output.

Algorithm 1: Augmented subspace iteration algorithm on non-nested meshes

1. Solve the auxiliary linear source problem: Find $\widetilde{u}_h^{(\ell+1)} \in V_h$, such that

$$a(\widetilde{u}_h^{(\ell+1)}, v_h) + (\zeta |u_h^{(\ell)}|^2 \widetilde{u}_h^{(\ell+1)}, v_h) = \lambda_h^{(\ell)} b(u_h^{(\ell)}, v_h), \quad \forall v_h \in V_h. \tag{3.1}$$

2. Define the augmented subspace $V_{H,h} := V_H + \mathrm{span}\{\widetilde{u}_h^{(\ell+1)}\}$ and solve the nonlinear eigenvalue problem: Find $(\lambda_h^{(\ell+1)}, u_h^{(\ell+1)}) \in \mathbb{R} \times V_{H,h}$ such that $b(u_h^{(\ell+1)}, u_h^{(\ell+1)}) = 1$ and

$$\widehat{a}(u_h^{(\ell+1)}, v_{H,h}) = \lambda_h^{(\ell+1)} b(u_h^{(\ell+1)}, v_{H,h}), \quad \forall v_{H,h} \in V_{H,h}. \tag{3.2}$$

The output $(\lambda_h^{(\ell+1)}, u_h^{(\ell+1)})$ is chosen such that $\lambda_h^{(\ell+1)}$ is the smallest one among all eigenvalues of (3.2).

Summarize the above-mentioned two steps by defining

$$(\lambda_h^{(\ell+1)}, u_h^{(\ell+1)}) = \texttt{AugSubspace}(V_H, V_h, \lambda_h^{(\ell)}, u_h^{(\ell)}).$$

Now we come to give the convergence analysis and the estimation of computational work for Algorithm 3.1.

Theorem 3.1 *Assume there exists an exact eigenpair (λ, u) such that the given eigenpair approximation $(\lambda_h^{(\ell)}, u_h^{(\ell)})$ satisfies the following error estimate*

$$|\lambda_h^{(\ell)} - \lambda| + \|u_h^{(\ell)} - u\|_0 \le C\rho(V_H)\|u_h^{(\ell)} - u\|_a. \tag{3.3}$$

Then the eigenpair approximation $(\lambda_h^{(\ell+1)}, u_h^{(\ell+1)})$ obtained by Algorithm 3.1 satisfies

$$\|u - u_h^{(\ell+1)}\|_a \le \gamma \|u - u_h^{(\ell)}\|_a + \kappa \|u - P_h u\|_a, \tag{3.4}$$

$$|\lambda_h^{(\ell+1)} - \lambda| + \|u_h^{(\ell+1)} - u\|_0 \le C\rho(V_H)\|u_h^{(\ell+1)} - u\|_a, \tag{3.5}$$

where γ and κ are defined as follows

$$\gamma = \frac{C\rho(V_H)}{1 - C\rho(V_{H,h})}, \qquad \kappa = \frac{1}{1 - C\rho(V_H)}, \tag{3.6}$$

where C is defined in (3.10).

Proof From (2.8), (3.1), the triangle inequality and setting $w_h = \widetilde{u}_h^{(\ell+1)} - P_h u$, we have

$$\begin{aligned} &a(\widetilde{u}_h^{(\ell+1)} - P_h u, w_h) + \left(\zeta |u_h^{(\ell)}|^2 (\widetilde{u}_h^{(\ell+1)} - P_h u), w_h\right) \\ &= b(\lambda_h^{(\ell)} u_h^{(\ell)}, w_h) - \left(a(u, w_h) + (\zeta |u_h^{(\ell)}|^2 P_h u, w_h)\right) \\ &= b(\lambda_h^{(\ell)} u_h^{(\ell)} - \lambda u, w_h) + \left(\zeta \left(|u|^2 u - \zeta |u_h^{(\ell)}|^2 P_h u\right), w_h\right) \end{aligned}$$

$$\leq C\|\lambda_h^{(\ell)}u_h^{(\ell)} - \lambda u\|_0\|w_h\|_0 + \left|\left(\zeta\left(|u|^2 - |u_h^{(\ell)}|^2\right)u, w_h\right)\right|.$$
$$+\left|\left(\zeta|u_h^{(\ell)}|^2(u - P_h u), w_h\right)\right| \tag{3.7}$$

For the second term of (3.7), using the Hölder inequality and Sobolev imbedding theorem,

$$\begin{aligned}
&\left(\zeta\left(|u|^2 - |u_h^{(\ell)}|^2\right)u, w_h\right) = \left(\zeta\left(u + u_h^{(\ell)}\right)\left(u - u_h^{(\ell)}\right)u, w_h\right)\\
&\leq \zeta\left(\int_\Omega |u + u_h^{(\ell)}|^6 \mathrm{d}\Omega\right)^{1/6}\left(\int_\Omega |u - u_h^{(\ell)}|^2 \mathrm{d}\Omega\right)^{1/2}\left(\int_\Omega |u|^6 \mathrm{d}\Omega\right)^{1/6}\left(\int_\Omega |w_h|^6 \mathrm{d}\Omega\right)^{1/6}\\
&\leq \zeta\|u + u_h^{(\ell)}\|_{0,6}\|u\|_{0,6}\|u - u_h^{(\ell)}\|_0\|w_h\|_{0,6}\\
&\leq C_3\|u - u_h^{(\ell)}\|_0\|w_h\|_a,
\end{aligned} \tag{3.8}$$

where $C_3 = C_\Omega^3\zeta(\|u\|_a + \|u_h^{(\ell)}\|_a)\|u\|_a$.

In the same way, for the third term of (3.7), we have

$$\left(\zeta|u_h^{(\ell)}|^2(u - P_h u), w_h\right) \leq C_4\|u - P_h u\|_0\|w_h\|_a, \tag{3.9}$$

where $C_4 = C_\Omega^3\zeta\|u_h^{(\ell)}\|_a^2$.

Combing (3.7), (3.8), (3.9) and Lemma 2.1, we have

$$\begin{aligned}
\|\widetilde{u}_h^{(\ell+1)} - P_h u\|_a &\leq \|u_h^{(\ell)}\|_0|\lambda - \lambda_h^{(\ell)}| + (C_3 + |\lambda|)\|u - u_h^{(\ell)}\|_0 + C_4\|u - P_h u\|_0\\
&\leq C\rho(V_h)\|u - \bar{u}_h\|_a,
\end{aligned} \tag{3.10}$$

where the constant C depends on C_3 and C_4, but independent of the mesh sizes.

From (3.10) and the triangle inequality, the following estimates hold

$$\begin{aligned}
\|u - \widetilde{u}_h^{(\ell+1)}\|_a &\leq \|u - P_h u\|_a + \|P_h u - \widetilde{u}_h^{(\ell+1)}\|_a\\
&\leq \|u - P_h u\|_a + C\rho(V_h)\|u - u_h^{(\ell)}\|_a.
\end{aligned} \tag{3.11}$$

Now we come to estimate the error for the eigenpair solution $(\lambda_h^{(\ell+1)}, u_h^{(\ell+1)})$ of problem (3.2). Since $V_{H,h}$ is a subset of V, (3.2) can be regarded as a subspace approximation to the problem (2.1). Then based on the definition of $V_{H,h}$, the subspace approximation results from Lemma 2.1 and Corollary 2.2, the following estimates hold

$$\begin{aligned}
\|u - u_h^{(\ell+1)}\|_a &\leq \frac{1}{1 - C\rho(V_{H,h})}\inf_{v_{H,h}\in V_{H,h}}\|u - v_{H,h}\|_a\\
&\leq \frac{1}{1 - C\rho(V_H)}\|\widetilde{u}_h^{(\ell+1)} - u\|_a\\
&\leq \frac{1}{1 - C\rho(V_H)}\left(\widetilde{C}\rho(V_H)\|u - u_h^{(\ell)}\|_a + \|u - P_h u\|_a\right)\\
&\leq \frac{C\rho(V_H)}{1 - C\rho(V_H)}\|u - u_h^{(\ell)}\|_a + \frac{1}{1 - C\rho(V_H)}\|u - P_h u\|_a,
\end{aligned} \tag{3.12}$$

where we used the inequality $\rho(V_{H,h}) \leq \rho(V_H)$ since $V_H \subset V_{H,h}$. The estimate (3.4) is the direct results of (3.12), thus (3.5) is readily proved by Lemma 2.1. □

Remark 3.1 Since $V_H \not\subset V_h$, the augmented subspace method defined by Algorithm 3.1 could be combined with the moving mesh method where the sequence of meshes does not have a nested relationship. This is the most important contribution of this paper. Since $V_H \not\subset V_h$,

the definition of the interpolation operator $I_H^h : V_H \to V_h$ is different from the standard one which is defined on the sequence of nested meshes. For the detailed implementation of the interpolation between the two non-nested meshes, please refer to the documentation of the finite element package FreeFem++ (c.f. [27]).

3.2 Efficient Implementation

In order to solve the nonlinear eigenvalue problem (3.2) (Step 2 of Algorithm 3.1) efficiently, we use the method proposed in [47]. For simplicity of notation, we omit the upper index ℓ, i.e. using $\widetilde{u}_h$ to denote $\widetilde{u}_h^{(\ell)}$. Let $\{\phi_{i,H}\}_{1\le i\le N_H}$ denote the Lagrange basis function for the coarse finite element space V_H, where $N_H := \dim V_H$ and $N_h := \dim V_h$.

Since (3.2) is a nonlinear eigenvalue problem, we need to use some type of nonlinear iteration method, such as the fixed point (self-consistent field) iteration. In each nonlinear iteration, the main work is to assemble the matrices for the problem (3.2) which is defined on the special space $V_{H,h}$. The function in $V_{H,h}$ can be denoted by $u_{H,h} = u_H + \alpha\widetilde{u}_h$. Solving problem (3.2) is to obtain the function $u_H \in V_H$ and the value $\alpha \in \mathbb{R}$. Set $u_H = \sum_{i=1}^{N_H} \mu_i \phi_{i,H}$ and $\mathbf{u}_H = [\mu_1, \cdots, \mu_{N_H}]^T \in \mathbb{R}^{N_H}$.

Based on the structure of the space $V_{H,h}$, the matrix version of the eigenvalue problem for (3.2) in each nonlinear iteration can be written as follows

$$\begin{pmatrix} A_H & b_{Hh} \\ b_{Hh}^T & \sigma \end{pmatrix} \begin{pmatrix} \mathbf{u}_H \\ \alpha \end{pmatrix} = \lambda_h \begin{pmatrix} M_H & c_{Hh} \\ c_{Hh}^T & \varrho \end{pmatrix} \begin{pmatrix} \mathbf{u}_H \\ \alpha \end{pmatrix}, \tag{3.13}$$

where $\mathbf{u}_H \in \mathbb{R}^{N_H}$ and $\alpha \in \mathbb{R}$.

It is obvious that the matrix M_H, the vector c_{Hh}, and the scalar ϱ keep the same during the nonlinear iteration process once $\widetilde{u}_h$ is obtained. However, the matrix A_H, the vector b_{Hh}, and the scalar σ change during the nonlinear iteration process. This subsection aims to introduce an efficient method to update A_H, b_{Hh} and σ which avoids computation on $\mathcal{T}_h$ during the nonlinear iteration process. This method is proposed in [47], however, for readers' easier understanding, we review it here.

From the definitions of the space $V_{H,h}$ and the definition of the eigenvalue problem (3.2), the matrix A_H has the following expansion

$$\begin{aligned}(A_H)_{i,j} &= \int_\Omega \nabla\phi_{i,H}\nabla\phi_{j,H}\mathrm{d}\Omega + \int_\Omega W\phi_{i,H}\phi_{j,H}\mathrm{d}\Omega + \int_\Omega \zeta(u_H + \alpha\widetilde{u}_h)^2\phi_{i,H}\phi_{j,H}\mathrm{d}\Omega \\ &:= (A_{H,1})_{i,j} + (A_{H,2})_{i,j},\end{aligned} \tag{3.14}$$

where

$$(A_{H,1})_{i,j} = \int_\Omega \nabla\phi_{i,H}\nabla\phi_{j,H}\mathrm{d}\Omega + \int_\Omega W\phi_{i,H}\phi_{j,H}\mathrm{d}\Omega, \tag{3.15}$$

and

$$\begin{aligned}(A_{H,2})_{i,j} &= \int_\Omega \zeta(u_H + \alpha\widetilde{u}_h)^2\phi_{i,H}\phi_{j,H}\mathrm{d}\Omega \\ &= \int_\Omega \zeta\big((u_H)^2 + 2\alpha u_H\widetilde{u}_h + \alpha^2(\widetilde{u}_h)^2\big)\phi_{i,H}\phi_{j,H}\mathrm{d}\Omega \\ &= \int_\Omega \zeta(u_H)^2\phi_{i,H}\phi_{j,H}\mathrm{d}\Omega + 2\alpha\int_\Omega \zeta\widetilde{u}_h u_H\phi_{i,H}\phi_{j,H}\mathrm{d}\Omega + \alpha^2\int_\Omega \zeta(\widetilde{u}_h)^2\phi_{i,H}\phi_{j,H}\mathrm{d}\Omega \\ &:= (A_{H,2,1})_{i,j} + 2\alpha(A_{H,2,2})_{i,j} + \alpha^2(A_{H,2,3})_{i,j}.\end{aligned} \tag{3.16}$$

It is obvious that the computational work for the matrix $(A_{H,2,1})_{i,j}$ is $\mathcal{O}(N_H)$. The matrices $A_{H,1}$ and $A_{H,2,3}$ do not change during the nonlinear iteration process.

Then the matrix $A_{H,2,2}$ has following expansion

$$(A_{H,2,2})_{i,j} = \sum_{k=1}^{N_H} \mu_k \int_\Omega \zeta \widetilde{u}_h \phi_{k,H} \phi_{i,H} \phi_{j,H} \mathrm{d}\Omega. \tag{3.17}$$

The expansion (3.17) gives a hint to define a tensor T_H as follows

$$(T_H)_{i,j,k} = \int_\Omega \zeta \widetilde{u}_h \phi_{k,H} \phi_{i,H} \phi_{j,H} \mathrm{d}\Omega. \tag{3.18}$$

Then the matrix $A_{H,2,2}$ has the following computational scheme

$$A_{H,2,2} = T_H \cdot \mathbf{u}_H, \tag{3.19}$$

where $T_H \cdot \mathbf{u}_H$ denotes the multiplication of the tensor T_H and the vector $\mathbf{u}_H$ corresponding to the last index k. From (3.18), the dimension of the tensor T_H is $N_H \times N_H \times N_H$ and the number of nonzero elements is $\mathcal{O}(N_H)$. Thus T_H is a sparse tensor and the computational work for the operation (3.19) is $\mathcal{O}(N_H)$.

Now, let us consider the computation for the vector b_{Hh} which has the following expansion

$$\begin{aligned}(b_{Hh})_i = &\int_\Omega \nabla \widetilde{u}_h \nabla \phi_{i,H} \mathrm{d}\Omega + \int_\Omega W \widetilde{u}_h \phi_{i,H} \mathrm{d}\Omega + \int_\Omega (u_H + \alpha \widetilde{u}_h)^2 \widetilde{u}_h \phi_{i,H} \mathrm{d}\Omega := (b_{Hh,1})_i \\ &+ (b_{Hh,2})_i,\end{aligned}$$

where

$$(b_{Hh,1})_i = \int_\Omega \nabla \widetilde{u}_h \nabla \phi_{i,H} \mathrm{d}\Omega + \int_\Omega W \widetilde{u}_h \phi_{i,H} \mathrm{d}\Omega, \tag{3.20}$$

and

$$\begin{aligned}(b_{Hh,2})_i &= \int_\Omega \zeta (u_H + \alpha \widetilde{u}_h)^2 \widetilde{u}_h \phi_{i,H} \mathrm{d}\Omega \\ &= \int_\Omega \zeta \left((u_H)^2 + 2\alpha \widetilde{u}_h u_H + \alpha^2 (\widetilde{u}_h)^2\right) \widetilde{u}_h \phi_{i,H} \mathrm{d}\Omega \\ &= \int_\Omega \zeta (u_H)^2 \widetilde{u}_h \phi_{i,H} \mathrm{d}\Omega + 2\alpha \int_\Omega \zeta (\widetilde{u}_h)^2 u_H \phi_{i,H} \mathrm{d}\Omega + \alpha^2 \int_\Omega \zeta (\widetilde{u}_h)^3 \phi_{i,H} \mathrm{d}\Omega \\ &:= (b_{Hh,2,1})_i + 2\alpha (b_{Hh,2,2})_i + \alpha^2 (b_{Hh,2,3})_i.\end{aligned} \tag{3.21}$$

The vector $b_{Hh,1}$ does not change during the nonlinear iteration process. Thus, we are left to consider the computation of the vector $b_{Hh,2}$.

First, the computation for the vector $b_{Hh,2,1}$ is treated as follows

$$(b_{Hh,2,1})_i = \int_\Omega \left(\sum_{j=1}^{N_H} u_j \phi_{j,H} \right)^2 \widetilde{u}_h \phi_{i,H} \mathrm{d}\Omega = \sum_{j=1}^{N_H} \sum_{k=1}^{N_H} \mu_j \mu_k \int_\Omega \widetilde{u}_h \phi_{j,H} \phi_{k,H} \phi_{i,H} \mathrm{d}\Omega. \tag{3.22}$$

Based on the tensor T_H, the vector $b_{Hh,2,1}$ can be calculated by the tensor multiplication

$$b_{Hh,2,1} = (T_H \cdot \mathbf{u}_H) \cdot \mathbf{u}_H = A_{H,2,2} \mathbf{u}_H, \tag{3.23}$$

and the computational work of the operation (3.23) is $\mathcal{O}(N_H)$.

Then the computation for $b_{Hh,2,2}$ can be done as follows

$$(b_{Hh,2,2})_i = \sum_{j=1}^{N_H} \mu_j \int_\Omega \zeta(\widetilde{u}_h)^2 \phi_{j,H}\phi_{i,H}\mathrm{d}\Omega = (A_{H,2,3}\mathbf{u}_H)_i. \tag{3.24}$$

Finally, the vector $b_{Hh,2,3}$ does not change during the nonlinear iteration process. For the computation of σ, we first have the following expansion

$$\begin{aligned}\sigma &= \int_\Omega |\nabla\widetilde{u}_h|^2 d\Omega + \int_\Omega W(\widetilde{u}_h)^2\mathrm{d}\Omega + \int_\Omega \zeta(u_H+\alpha\widetilde{u}_h)^2(\widetilde{u}_h)^2\mathrm{d}\Omega \\ &= \int_\Omega \big(|\nabla\widetilde{u}_h|^2 + W(\widetilde{u}_h)^2\big)\mathrm{d}\Omega + \int_\Omega \zeta\big((u_H)^2 + 2\alpha u_H\widetilde{u}_h + \alpha^2(\widetilde{u}_h)^2\big)(\widetilde{u}_h)^2\mathrm{d}\Omega \\ &:= d_1 + d_2,\end{aligned} \tag{3.25}$$

where

$$d_1 = \int_\Omega \big(|\nabla\widetilde{u}_h|^2 + W(\widetilde{u}_h)^2\big)\mathrm{d}\Omega, \tag{3.26}$$

and

$$\begin{aligned}d_2 &= \sum_{i=1}^{N_H}\sum_{j=1}^{N_H}\mu_i\mu_j\int_\Omega \zeta(\widetilde{u}_h)^2\phi_{i,H}\phi_{j,H}\mathrm{d}\Omega + 2\alpha\sum_{i=1}^{N_H}\mu_i\int_\Omega\zeta(\widetilde{u}_h)^3\phi_{i,H}\mathrm{d}\Omega \\ &\quad +\alpha^2\int_\Omega\zeta(\widetilde{u}_h)^4\mathrm{d}\Omega \\ &= \mathbf{u}_H^T A_{H,2,3}\mathbf{u}_H + 2\alpha\mathbf{u}_H^T b_{Hh,2,3} + \alpha^2\sigma_h,\end{aligned} \tag{3.27}$$

with the scalar σ_h being defined by

$$\sigma_h = \int_\Omega \zeta(\widetilde{u}_h)^4\mathrm{d}\Omega. \tag{3.28}$$

Remark 3.2 The computational cost of assembling the tensor, matrices, vectors, and scalar is $\mathcal{O}(N_h)$, however, that for each nonlinear iteration step is only $\mathcal{O}(M_H)$, where M_H is the computational cost for solving the eigenvalue problem (3.2) with $M_H \ll N_h$. Assume it needs ϖ nonlinear iterations for (3.2), the computational cost is $\mathcal{O}(N_h + \varpi M_H)$ for Algorithm 3.1 which is almost independent of ϖ.

4 Multilevel Correction Method on the *r*-Adaptive Meshes

In this section, based on the augmented subspace iteration algorithm (Algorithm 3.1), we design a multilevel correction type of adaptive finite element method for the nonlinear eigenvalue problem (2.1) on the sequence of r-adaptive meshes. To be specific, suppose a coarse mesh $\mathcal{T}_H$ is given and V_H is defined on $\mathcal{T}_H$. Then a sequence of meshes T_{h_k} $(k = 1, \cdots, n)$ is generated by the r-adaptive method with the help of mesh generation tools, such as *mshmet* and *mmg3d* [23, 25]. We then construct the corresponding linear finite element spaces V_{h_k} $(k = 1, \cdots, n)$ on $\mathcal{T}_{h_k}$. We assume the relationship between every pair of adjacent levels of linear finite element space as

$$N_k \approx \xi^d N_{k-1}, \tag{4.1}$$

$$\delta_{h_k}(u) \approx \frac{1}{\xi}\delta_{h_{k-1}}(u), \quad k = 2, \cdots, n, \tag{4.2}$$

where ξ is called the refinement constant and $N_k := \dim V_{h_k}$.

The corresponding multilevel correction method is described by Algorithm 4.

Algorithm 2: Multilevel correction method on r-adaptive meshes

1. Solve the eigenvalue problem on V_{h_1}: Find $(\lambda_{h_1}, u_{h_1}) \in \mathbb{R} \times V_{h_1}$ such that

$$\widehat{a}(u_{h_1}, v_{h_1}) = \lambda_{h_1} b(u_{h_1}, v_{h_1}), \quad \forall v_{h_1} \in V_{h_1}. \tag{4.3}$$

2. For $k = 2, \cdots, n$, do the following iteration:
   (a) Generate the mesh $\mathcal{T}_{h_k}$ by $(\lambda_{h_{k-1}}, u_{h_{k-1}})$ using the r-adaptive method such that the property (4.2) holds.
   (b) Set $(\lambda_{h_k}^{(0)}, u_{h_k}^{(0)}) = (\lambda_{h_{k-1}}, u_{h_{k-1}})$.
   (c) For $\ell = 0, \cdots, m-1$, do the 'augmented subspace iteration algorithm on non-nested meshes'

$$(u_{h_k}^{(\ell+1)}, \lambda_{h_k}^{(\ell+1)}) = \texttt{AugSubspace}(V_H, V_h, \lambda_{h_k}^{(\ell)}, u_{h_k}^{(\ell)}).$$

   (d) Set $(\lambda_{h_k}, u_{h_k}) = (\lambda_{h_k}^{(m)}, u_{h_k}^{(m)})$.

Based on Lemma 2.1, Corollary 2.2, Theorem 3.1 and the property (4.2), we deduce the error estimate for Algorithm 4 by recursive argument.

Theorem 4.1 *Under the condition of (4.2), the eigenpair approximation $(\lambda_{h_n}, u_{h_n}) \in \mathbb{R} \times V_{h_n}$ obtained by Algorithm 4 and $E_{h_n} = E(u_{h_n})$ have the following error estimates*

$$\|u - u_{h_n}\|_a \leq \frac{1 - (\xi\gamma^m)^n}{1 - (\xi\gamma^m)} \kappa \delta_{h_n}(u), \tag{4.4}$$

$$|\lambda_{h_n} - \lambda| + \|u_{h_n} - u\|_0 \leq C \frac{1 - (\xi\gamma^m)^n}{1 - (\xi\gamma^m)} \kappa \rho(V_H) \delta_{h_n}(u), \tag{4.5}$$

$$|E_{h_n} - E| \leq C \frac{1 - (\xi\gamma^m)^n}{1 - (\xi\gamma^m)} \kappa \rho(V_H) \delta_{h_n}(u), \tag{4.6}$$

under the condition $\xi\gamma^m < 1$.

Proof From Corollary 2.2 and the property $\rho(V_{h_1}) \leq \rho(V_H)$, the eigenfunction approximation u_{h_1} obtained by Step 1 of Algorithm 4 satisfies the following error estimates

$$\|u - u_{h_1}\|_a = \|u - \bar{u}_{h_1}\|_a \leq \frac{1}{1 - C\rho(V_{h_1})} \delta_{h_1}(u) \leq \kappa \|u - P_{h_1} u\|_a. \tag{4.7}$$

Combining Corollary 2.2, (4.7) and recursive argument leads to the following estimates

$$\begin{aligned}
\|u - u_{h_n}\|_a &= \|u - u_{h_n}^{(m)}\|_a \leq \gamma^m \|u - u_{h_n}^{(0)}\|_a + \kappa \|u - P_{h_n} u\|_a \\
&= \gamma^m \|u - u_{h_{n-1}}\|_a + \kappa \|u - P_{h_n} u\|_a \\
&\leq \gamma^m \left(\gamma^m \|u - u_{h_{n-2}}\|_a + \kappa \|u - P_{h_{n-1}} u\|_a\right) + \kappa \|u - P_{h_n} u\|_a \\
&\leq \gamma^{(n-1)m} \|u - u_{h_1}\|_a + \sum_{k=2}^{n} \gamma^{(n-k)m} \kappa \|u - P_{h_k} u\|_a
\end{aligned}$$

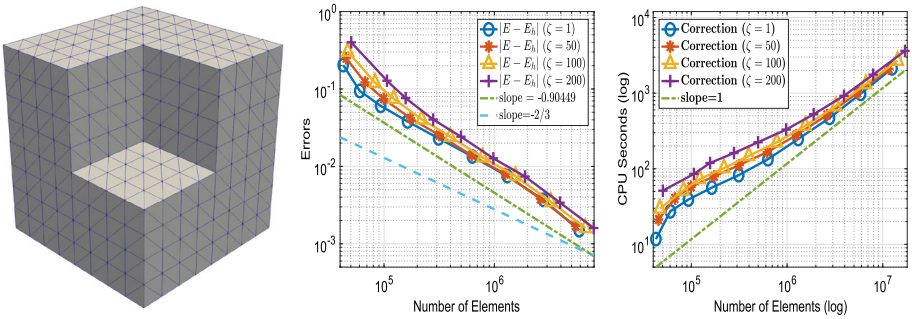

Fig. 1 The coarsest mesh, the error estimate and CPU time for Example 1 by Algorithm 4 with linear element

$$
\begin{aligned}
&\le \gamma^{(n-1)m}\kappa\|u - P_{h_1}u\|_a + \sum_{k=2}^{n}\gamma^{(n-k)m}\kappa\|u - P_{h_k}u\|_a \\
&\le \sum_{k=1}^{n}\gamma^{(n-k)m}\kappa\|u - P_{h_k}u\|_a = \sum_{k=1}^{n}\gamma^{(n-k)m}\kappa\delta_{h_k}(u) \\
&\le \left(\sum_{k=1}^{n}\gamma^{(n-k)m}\xi^{n-k}\right)\kappa\delta_{h_n}(u) = \left(\sum_{k=1}^{n}(\xi\gamma^m)^{n-k}\right)\kappa\delta_{h_n}(u) \\
&= \frac{1-(\xi\gamma^m)^n}{1-(\xi\gamma^m)}\kappa\delta_{h_n}(u). \qquad (4.8)
\end{aligned}
$$

For such choice of m, we arrive at the desired result (4.4), while (4.5) and (4.6) can be obtained by Lemma 2.1, Corollary 2.1 and (4.8). □

Now, we analyze the computational cost for Algorithm 4. Since the linear boundary value problem (3.1) in Algorithm 3.1 can be solved by a multigrid method, the computational cost for this part can be of optimal order.

The computational cost for the second step in Algorithm 3.1 is different from the linear eigenvalue problems [37, 42, 44]. In this step, we need to solve a nonlinear eigenvalue problem (3.2). Always, some type of nonlinear iteration method (self-consistent or Newton-type iteration) is adopted. In each nonlinear iteration, we need to assemble the matrix on the finite element space V_{H,h_k} $(k = 2, \ldots, n)$ which computational cost is $\mathcal{O}(N_k)$. Fortunately, assembling the matrix could be carried out in a parallel way easily since there is no data transfer.

Remark 4.1 Assume solving the eigenvalue problem (3.13) and nonlinear eigenvalue problem (4.3) in initial space V_{h_1} need work $\mathcal{O}(M_H)$ and $\mathcal{O}(M_{h_1})$, respectively, and the work for solving the source problem in V_{h_k} be $\mathcal{O}(N_k)$ for $k = 2, 3, \ldots, n$. Let ϖ denote the nonlinear iteration times when we solve the nonlinear eigenvalue problem (3.2). When we use the efficient implementing techniques in Subsection 3.2, the work involved in Algorithm 4 has the following estimate:

$$\text{Total work} = \mathcal{O}\left(N_n + \varpi M_H \ln N_n + M_{h_1}\right). \qquad (4.9)$$

Remark 4.2 Although the number of nonlinear iterations of Algorithm 3.1, i.e. ϖ, increases as the nonlinear strength increases (ζ increases), the computational cost is asymptotically optimal and almost independent of ϖ due to the fact $M_H \ll N_n$ and $M_{h_1} \le N_n$.

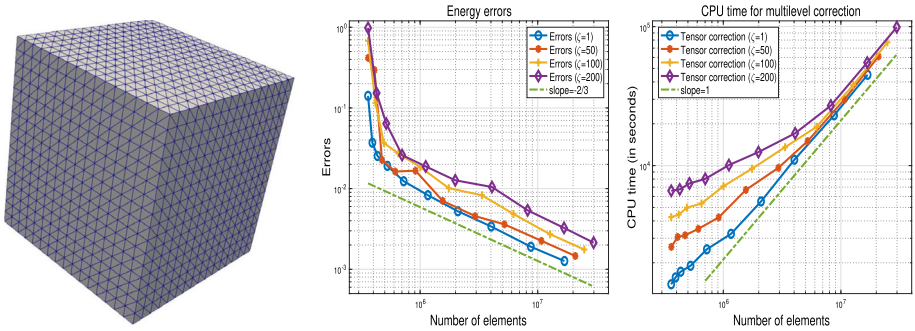

Fig. 2 The coarse and initial mesh, the energy errors and CPU time for Example 2 by Algorithm 4 with linear element

5 Numerical Experiments

This section provides three numerical examples to validate the proposed augmented subspace algorithm and the corresponding theoretical analysis. With the help of the finite element package FreeFem++ [27, 34], the numerical experiments are carried out on LSSC-IV in the State Key Laboratory of Scientific and Engineering Computing, Academy of Mathematics and Systems Science, Chinese Academy of Sciences. Each computing node has two 18-core Intel Xeon Gold 6140 processors at 2.3 GHz and 192 GB of memory.

The eigenvalue problem on the coarsest space and low dimensional subspace $V_{H,h}$ are solved by SLEPc [29] in parallel and serial ways, respectively. The linear equation (3.1) in Algorithm 3.1 is solved with the GAMG [2, 7] from PETSc [7]. Adaptive meshes are generated by *mshmet* and *mmg3d* [23, 25].

Example 1 We solve nonlinear eigenvalue (1.3) where

$$W = \frac{1}{2}(\gamma_x^2 x^2 + \gamma_y^2 y^2 + \gamma_z^2 z^2),$$

and $\gamma_x = \gamma_y = \gamma_z = 1$ on the L-shape domain $\Omega = (-1, 1)^3 \backslash [0, 1)^3$, with different choice of ζ.

Although the ground state of BECs is always not defined on the L-shape domain, this example is provided to show the ability of the r-adaptive method and the efficiency of the multilevel correction method. The coarsest mesh $\mathcal{T}_{h_1} := \mathcal{T}_H$ is presented in the left subfigure of Fig. 1. The corresponding numerical results for energy approximations and CPU time by Algorithm 4 are shown in Fig. 1, where Algorithm 4 is shown to achieve the optimal error and linear scale complexity. The CPU time results show that the computational cost of Algorithm 4 is independent of the strength of the nonlinearity.

Example 2 In this example, we consider the ground state solution of BEC with a harmonic oscillator potential of a stirrer corresponding to a far-blue detuned Gaussian laser beam [9], i.e.,

$$W = \frac{1}{2}(\gamma_x^2 x^2 + \gamma_y^2 y^2 + \gamma_z^2 z^2) + \omega e^{-\delta((x-r_0)^2+y^2)},$$

where $\gamma_x = \gamma_y = 1, \gamma_z = 2, \omega = 4, \delta = r_0 = 1$ and $\Omega = (-6, 6)^3$, with different choices of ζ.

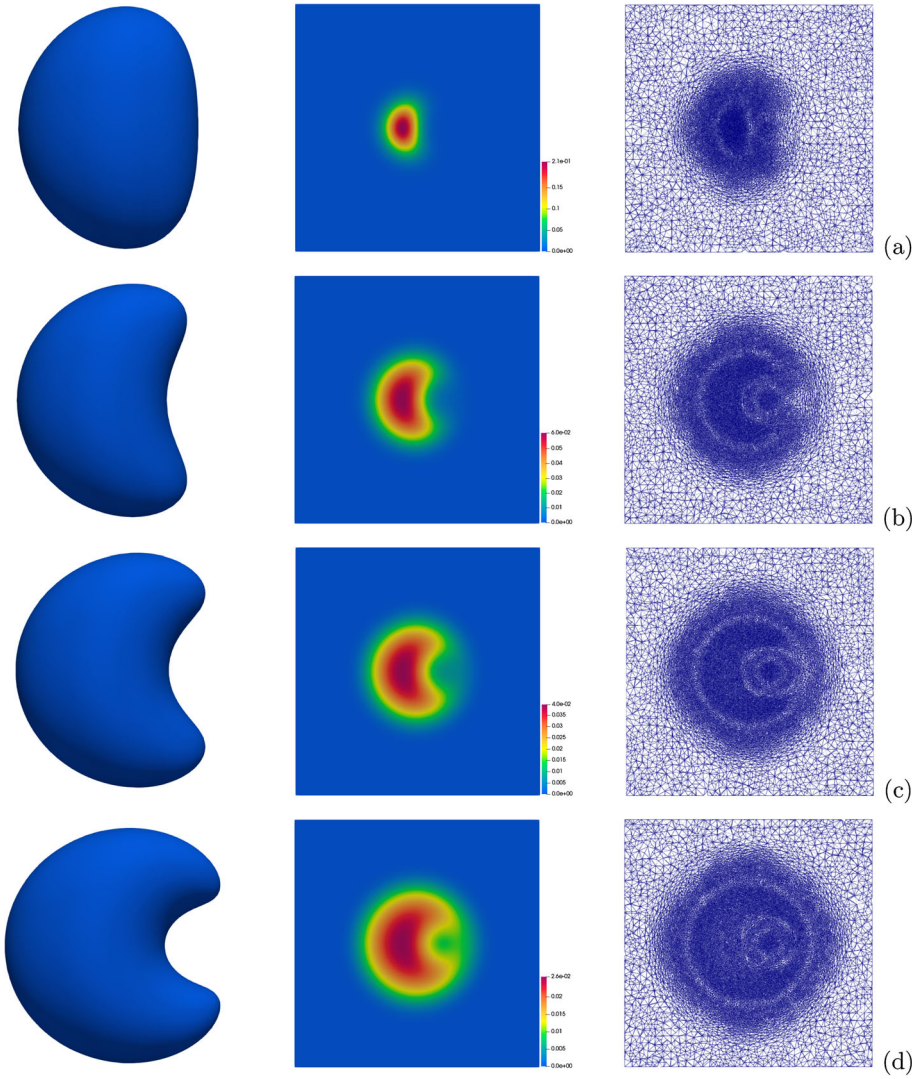

Fig. 3 Isosurfaces of $|u_h|^2$ (left column), their corresponding contour plot on the interior slice $z = 0$ (middle column) and the corresponding adaptive meshes (right column) by using linear elements in Example 2 for different ζ: **a** $\zeta = 1$, **b** $\zeta = 50$, **c** $\zeta = 100$, **d** $\zeta = 200$

We check the convergence and efficiency of Algorithm 4 with $\zeta = 1, 50, 100, 200$. The coarsest mesh is presented in the subfigure of Fig. 2. While the corresponding numerical results for energy approximations and CPU time by Algorithm 4 are shown in Fig. 2, where Algorithm 4 is shown to achieve the optimal error and the efficiency is independent of the strength of the nonlinearity. Figure 3 plots the isosurfaces of $|u_h|^2$, their contour plot on the interior slice $z = 0$, and adaptive mesh sections for different ζ.

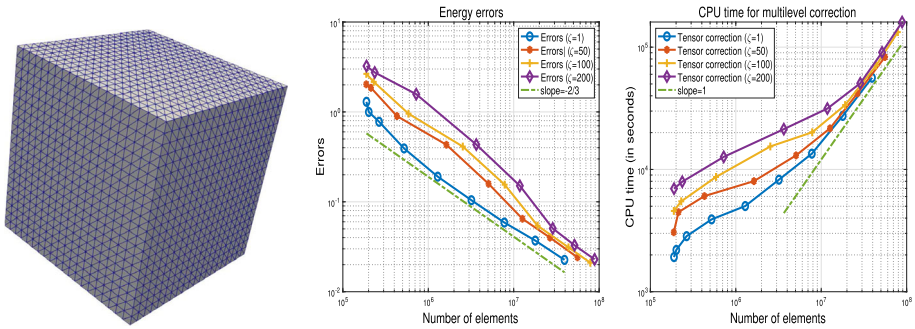

Fig. 4 The coarse and initial mesh, the error estimate and CPU time for Example 3 by Algorithm 4 with linear element

Example 3 In this example, we consider the ground state solution of BEC with optical lattice potential [10, 28] that is a more complex nonlinear eigenvalue, i.e.,

$$W = \frac{1}{2}(\gamma_x^2 x^2 + \gamma_y^2 y^2 + \gamma_z^2 z^2) + \delta\big(\sin^2(2\pi x) + \sin^2(2\pi y) + \sin^2(2\pi z)\big),$$

where $\gamma_x = \gamma_y = \gamma_z = 1$, $\delta = 50$ and $\Omega = (-6, 6)^3$, with different choice of ζ. We also check the convergence and efficiency of Algorithm 4 with $\zeta = 1, 50, 100, 200$.

The coarsest mesh is presented in the left subfigure of Fig. 4. Figure 4 shows the corresponding numerical results for energy approximations and CPU time by Algorithm 4. From Fig. 4, we can find that Algorithm 4 also achieve the optimal error and the efficiency is independent of the strength of the nonlinearity. The isosurfaces of $|u_h|^2$, their corresponding contour plot on the interior slice $z = 0$ and adaptive mesh sections for different ζ are shown in Fig. 5.

6 Concluding Remarks

In this paper, we design an efficient multilevel correction type of moving mesh method for solving the ground state solution of Bose–Einstein condensates. In addition, the tensor assembling technique from [44, 47] is adopted to improve efficiency. The corresponding convergence property and computational complexity are also presented. The proposed numerical method makes the computational work for solving the NLEP (1.3) be asymptotically the same as solving the corresponding linear boundary value problem by the moving mesh method.

Based on the result of the computational work, the method in this paper provides a way to make the computational work escape from the dependence on the nonlinearity strength of the problem. The idea and method here can be extended to other nonlinear problems such as the ground state of rotating dipolar BEC and the Kohn-Sham equation.

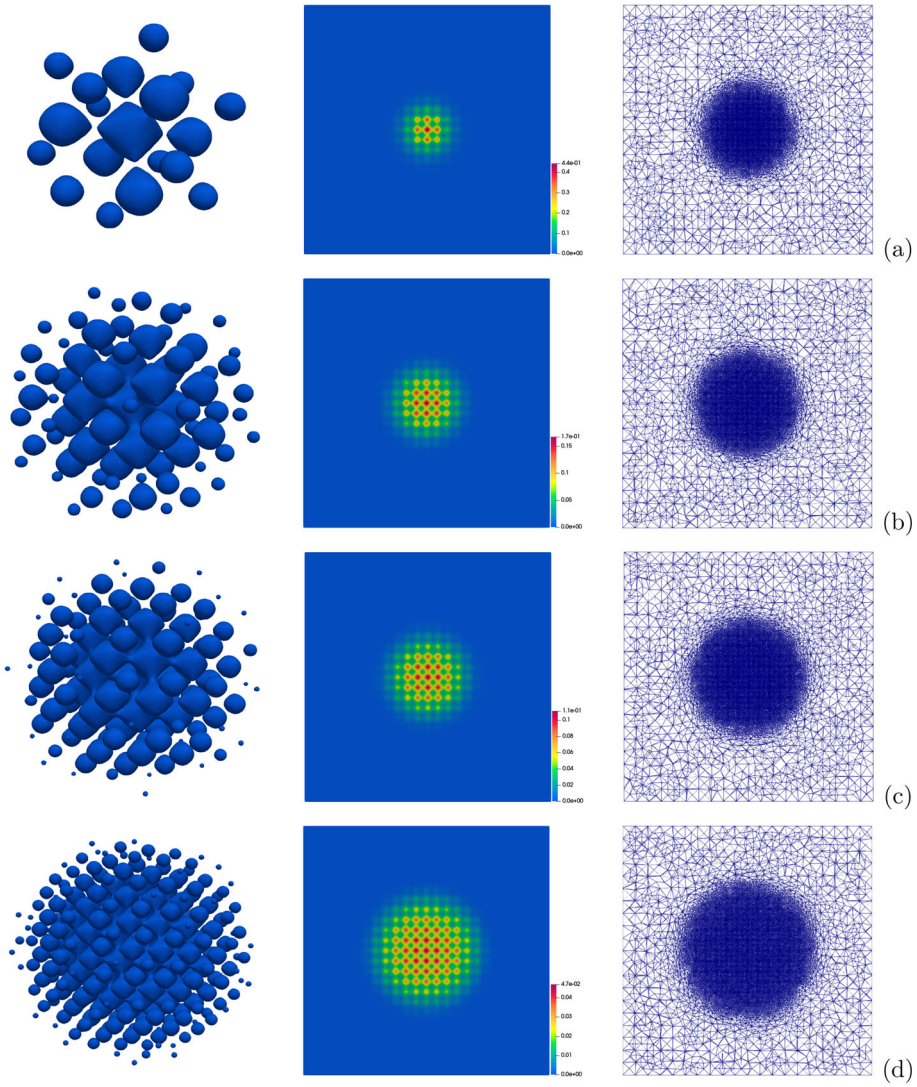

Fig. 5 Isosurfaces (left column), their contour plot on the interior slice $z = 0$ (middle column) and adaptive mesh sections (right column) for ground state solutions in Example 3 for different ζ: **a** $\zeta = 1$, **b** $\zeta = 50$, **c** $\zeta = 100$, **d** $\zeta = 200$

Acknowledgements The authors would like to thank both referees for their valuable comments and helpful suggestions that improved this paper.

Funding The first author (H. Xie) was supported in part by the National Key Research and Development Program of China (2019YFA0709601), Beijing Natural Science Foundation (Z200003) and the National Center for Mathematics and Interdisciplinary Science, CAS. The second author (M. Xie) was supported in part by the National Natural Science Foundation of China (Nos. 12001402, 12071343, 12271400). The third author (X. Yin) was supported by the Hubei Provincial Science and Technology Innovation Base (Platform) Special Project (No. 2020DFH002).

Data Availability Enquiries about data availability should be directed to the authors.

Code Availability The code can be made available on reasonable request.

Declarations

Conflict of interest This work does not have any conflicts of interest.

References

1. Adams, R.A.: Sobolev Spaces. Academic Press, Adams (1975)
2. Adams, M.F., Bayraktar, H.H., Keaveny, T.M., Papadopoulos, P.: Ultrascalable implicit finite element analyses in solid mechanics with over a half a billion degrees of freedom, In: SC'04: Proceedings of the 2004 ACM/IEEE Conference on Supercomputing, pp. 34–34. IEEE (2004)
3. Alauzet, F., Frey, P.J.: Estimateur d'erreur géométrique et métriques anisotropes pour l'adaptation de maillage. Partie I: aspects théoriques. Rapport de recherche RR-4759. INRIA, (2003)
4. Anderson, M.H., Ensher, J.R., Matthews, M.R., Wieman, C.E., Cornell, E.A.: Observation of Bose–Einstein condensation in a dilute atomic vapor. Science **269**(5221), 198–201 (1995)
5. Antoine, X., Levitt, A., Tang, Q.: Efficient spectral computation of the stationary states of rotating Bose–Einstein condensates by preconditioned nonlinear conjugate gradient methods. J. Comput. Phys. **343**, 92–109 (2017)
6. Antoine, X., Tang, Q., Zhang, Y.: A preconditioned conjugated gradient method for computing ground states of rotating dipolar Bose–Einstein condensates via kernel truncation method for dipole–dipole interaction evaluation. Commun. Comput. Phys. **24**(4), 966–988 (2018)
7. Balay, S., Abhyankar, S., Adams, M., Brown, J. et. al.: PETSc users manual revision 3.8, Technical report, Argonne National Lab. (ANL), Argonne, IL (United States) (2017)
8. Bao, W., Cai, Y.: Mathematical theory and numerical methods for Bose–Einstein condensation. Kinet. Relat. Models **6**(1), 1–135 (2013)
9. Bao, W., Du, Q.: Computing the ground state solution of Bose–Einstein condensates by a normalized gradient flow. SIAM J. Sci. Comput. **25**(5), 1674–1697 (2004)
10. Bao, W., Chern, I.-L., Lim, F.-Y.: Efficient and spectrally accurate numerical methods for computing ground and first excited states in Bose–Einstein condensates. J. Comput. Phys. **219**(2), 836–854 (2006)
11. Bao, G., Hu, G., Liu, D.: Numerical solution of the Kohn–Sham equation by finite element methods with an adaptive mesh redistribution technique. J. Sci. Comput. **55**(2), 372–391 (2013)
12. Beckett, G., MacKenzie, J., Robertson, M.L.: An r-adaptive finite element method for the solution of the two-dimensional phase-field equations. Commun. Comput. Phys. **1**(5), 805–826 (2006)
13. Brenner, S., Scott, R.: The Mathematical Theory of Finite Element Methods, vol. 15. Springer Science & Business Media, Berlin (2007)
14. Cancès, E., Chakir, R., Maday, Y.: Numerical analysis of nonlinear eigenvalue problems. J. Sci. Comput. **45**(1–3), 90–117 (2010)
15. Cancès, E., Dusson, G., Maday, Y., Stamm, B., Vohralík, M.: A perturbation-method-based a posteriori estimator for the planewave discretization of nonlinear Schrödinger equations. C. R. Math. **352**(11), 941–946 (2014)
16. Cancès, E., Chakir, R., He, L., Maday, Y.: Two-grid methods for a class of nonlinear elliptic eigenvalue problems. IMA J. Numer. Anal. **38**(2), 605–645 (2018)
17. Chen, H.-S., Chang, S.-L., Chien, C.-S.: Spectral collocation methods using sine functions for a rotating Bose–Einstein condensation in optical lattices. J. Comput. Phys. **231**(4), 1553–1569 (2012)
18. Chien, C.-S., Jeng, B.W.: A two-grid discretization scheme for semilinear elliptic eigenvalue problems. SIAM J. Sci. Comput. **27**(4), 1287–1304 (2006)
19. Chien, C.-S., Huang, H.-T., Jeng, B.-W., Li, Z.-C.: Two-grid discretization schemes for nonlinear Schrödinger equations. J. Comput. Appl. Math. **214**(2), 549–571 (2008)
20. Ciarlet, P.G.: The Finite Element Method for Elliptic Problems. SIAM, New Delhi (2002)
21. Danaila, I., Kazemi, P.: A new Sobolev gradient method for direct minimization of the Gross–Pitaevskii energy with rotation. SIAM J. Sci. Comput. **32**(5), 2447–2467 (2010)
22. Danaila, I., Protas, B.: Computation of ground states of the Gross–Pitaevskii functional via Riemannian optimization. SIAM J. Sci. Comput. **39**(6), B1102–B1129 (2017)
23. Dapogny, C., Dobrzynski, C., Frey, P.: Three-dimensional adaptive domain remeshing, implicit domain meshing, and applications to free and moving boundary problems. J. Comput. Phys. **262**, 358–378 (2014)

24. Davis, K.B., Mewes, M., Andrews, M.R., van Druten, N.J., Durfee, D.S., Kurn, D.M., Ketterle, W.: Bose–Einstein condensation in a gas of sodium atoms. Phys. Rev. Lett. **75**(22), 3969 (1995)
25. Frey, P.-J., Alauzet, F.: Anisotropic mesh adaptation for CFD computations. Comput. Methods Appl. Mech. Eng. **194**(48–49), 5068–5082 (2005)
26. García-Ripoll, J.J., Pérez-García, V.M.: Optimizing Schrödinger functionals using Sobolev gradients: Applications to quantum mechanics and nonlinear optics. SIAM J. Sci. Comput. **23**(4), 1316–1334 (2001)
27. Hecht, F.: New development in FreeFem++. J. Numer. Math. **20**(3–4), 251–266 (2012)
28. Heid, P., Stamm, B., Wihler, T.P.: Gradient flow finite element discretizations with energy-based adaptivity for the Gross–Pitaevskii equation. J. Comput. Phys. **436**, 110165 (2021)
29. Hernandez, V., Roman, J.E., Vidal, V.: SLEPc: A scalable and flexible toolkit for the solution of eigenvalue problems. ACM Trans. Math. Softw. (TOMS) **31**(3), 351–362 (2005)
30. Hu, G., Zegeling, P.A.: Simulating finger phenomena in porous media with a moving finite element method. J. Comput. Phys. **230**(8), 3249–3263 (2011)
31. Hu, G., Qiao, Z., Tang, T.: Moving finite element simulations for reaction-diffusion systems. Adv. Appl. Math. Mech. **4**(3), 365–381 (2012)
32. Jeng, B.W., Chien, C.S., Chern, I.L.: Spectral collocation and a two-level continuation scheme for dipolar Bose–Einstein condensates. J. Comput. Phys. **256**, 713–727 (2014)
33. Jia, S., Xie, H., Xie, M., Xu, F.: A full multigrid method for nonlinear eigenvalue problems. Sci. China Math. **59**(10), 2037–2048 (2016)
34. Jolivet, P., Hecht, F., Nataf, F., Prud'Homme, C.: Scalable domain decomposition preconditioners for heterogeneous elliptic problems. Sci. Program. **22**(2), 157–171 (2014)
35. Li, X.-G., Zhu, J., Zhang, R.-P., Cao, S.: A combined discontinuous Galerkin method for the dipolar Bose–Einstein condensation. J. Comput. Phys. **275**, 363–376 (2014)
36. Lieb, E.H., Seiringer, R., Yngvason, J.: Bosons in a trap: A rigorous derivation of the Gross–Pitaevskii energy functional. Phys. Rev. A **61**, 043602 (2000)
37. Lin, Q., Xie, H.: A multi-level correction scheme for eigenvalue problems. Math. Comput. **84**(291), 71–88 (2015)
38. Tang, T.: Moving mesh methods for computational fluid dynamics. Contemp. Math. **383**(8), 141–173 (2005)
39. van Dam, A., Zegeling, P.A.: A robust moving mesh finite volume method applied to 1D hyperbolic conservation laws from magnetohydrodynamics. J. Comput. Phys. **216**(2), 526–546 (2006)
40. Wang, H., Li, R., Tang, T.: Efficient computation of dendritic growth with r-adaptive finite element methods. J. Comput. Phys. **227**(12), 5984–6000 (2008)
41. Wu, X., Wen, Z., Bao, W.: A regularized Newton method for computing ground states of Bose–Einstein condensates. J. Sci. Comput. **73**(1), 303–329 (2017)
42. Xie, H.: A multigrid method for eigenvalue problem. J. Comput. Phys. **274**, 550–561 (2014)
43. Xie, H.: A multigrid method for nonlinear eigenvalue problems. Sci Sin. (Mathematica) **45**, 1193–1204 (2015)
44. Xie, H., Xie, M.: A multigrid method for ground state solution of Bose–Einstein condensates. Commun. Comput. Phys. **19**(3), 648–662 (2016)
45. Xie, H., Xie, M.: Computable error estimates for ground state solution of Bose–Einstein condensates. J. Sci. Comput. **81**(2), 1072–1087 (2019)
46. Xu, F.: A cascadic adaptive finite element method for nonlinear eigenvalue problems in quantum physics. Multiscale Model. Simul. **18**(1), 198–220 (2020)
47. Zhang, N., Xu, F., Xie, H.: An efficient multigrid method for ground state solution of Bose–Einstein condensates. Int. J. Numer. Anal. Model. **16**(5), 789–803 (2019)
48. Zhou, A.: An analysis of finite-dimensional approximations for the ground state solution of Bose–Einstein condensates. Nonlinearity **17**(2), 541–550 (2004)